tration of $3.8 \times 10^{18}\,cm^{-3}$ and an electron mobility of $1450\,cm^2/Vs$. These values were almost identical to those of Si-doped GaAs on the (100) substrate grown in the same run with $4.1 \times 10^{18}\,cm^{-3}$ and $1620\,cm^2/Vs$, respectively. As can be seen in Fig. 1, the electron concentration of the (311)A

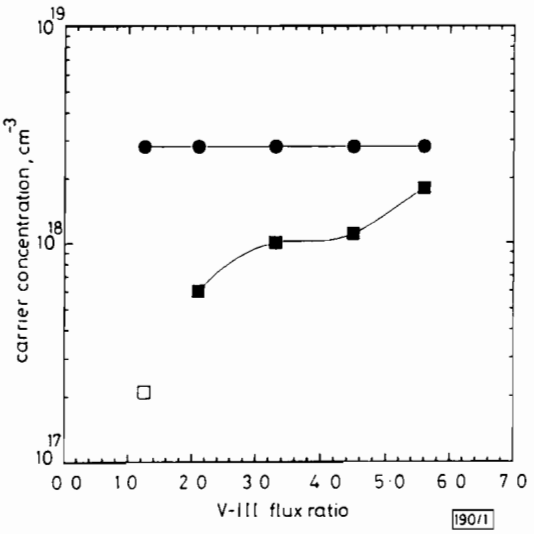

Fig. 1 *Carrier type and concentration of (100) and (311)A sample as function of V/III flux ratio*

■ (311)A *n*-type
□ (311)A *p*-type
● (100) *n*-type

sample varied from $6.0 \times 10^{17}\,cm^{-3}$ to $1.8 \times 10^{18}\,cm^{-3}$ as the V/III flux ratio increased from 2.0 to 5.6 whereas that of the (100) sample was kept constant, which indicates that the compensation ratio can also be controlled only by the V/III flux ratio.

These results are interpreted as follows; there are two different kinds of sites on the surface of (311)A GaAs (Fig. 2). One is a double dangling-bond site seen on a conventional (100) surface, which is an As site and acts as an acceptor if occupied by Si. The other is a single dangling-bond site seen on the (111)A surface and it is a Ga site at which Si acts as a donor.

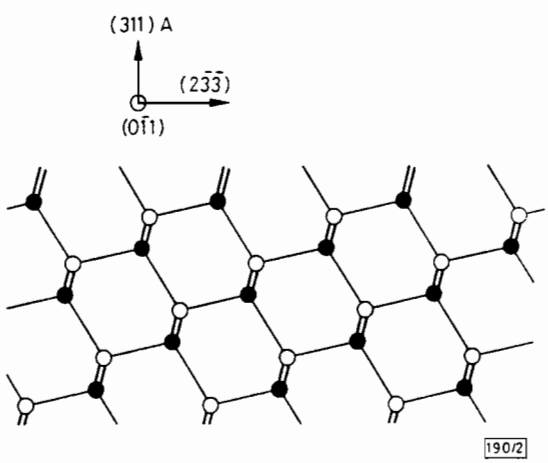

Fig. 2 *Schematic cross-sectional view of ideal (311)A GaAs surface*

○ Ga
● As

The density of these two sites are exactly the same on an ideal (311)A surface. The fact that Si acts as an acceptor at the low V/III flux ratio suggests that Si likes to occupy the As site with a double dangling-bond rather than the single dangling-bonded Ga site. It can be speculated that under the high V/III flux ratio, a large number of As molecules push Si away to the Ga site making it act as a donor. Therefore, the larger the V/III flux ratio, the more the Ga-sited Si exists, resulting in larger electron density as shown in Fig. 1.

In conclusion, we have demonstrated that the V/III flux ratio defines the conduction type of Si-doped GaAs grown by MBE on the (311)A substrate even at the growth temperature of 600°C. The dependence of the electron concentration on the V/III flux ratio was also shown. These results offer a new technique for many device applications.

T. TAKAMORI
K. WATANABE
T. FUKUNAGA

14th February 1991

Semiconductor Technology Laboratory
OKI Electric Industry Co., Ltd.
550-5 Higashiasakawa, Hachioji, Tokyo 193, Japan

References

1 CHAI, Y. G., CHOW, R., and WOOD, C. E. C.: 'The effect of growth conditions on Si incorporation in molecular beam epitaxial GaAs', *Appl. Phys. Lett.*, 1981, **39**, pp. 800–803
2 BALLINGALL, J. M., and WOOD, C. E. C.: 'Crystal orientation dependence of silicon autocompensation in molecular beam epitaxial gallium arsenide', *Appl. Phys. Lett.*, 1982, **41**, pp. 947–949
3 WANG, W. I., MENDEZ, E. E., KUAN, T. S., and ESAKI, L.: 'Crystal orientation dependence of silicon doping in molecular beam epitaxial AlGaAs/GaAs heterostructures', *Appl. Phys. Lett.*, 1985, **47**, pp. 826–828
4 MILLER, D. L.: 'Lateral p–n junction formation in GaAs molecular beam epitaxy by crystal plane dependent doping', *Appl. Phys. Lett.*, 1985, **47**, pp. 1309–1311
5 SUBBANNA, S., KROEMER, H., and MERZ, J. L.: 'Molecular-beam-epitaxial growth and selected properties of GaAs layers and GaAs/(Al, Ga)As superlattices with the (211) orientation', *J. Appl. Phys.*, 1986, **59**, pp. 488–494
6 TAKAMORI, T., FUKUNAGA, T., KOBAYASHI, J., ISHIDA, K., and NAKASHIMA, H.: 'Electrical and optical properties of Si doped GaAs grown by molecular beam epitaxy on (311) substrates', *Japanese J. Appl. Phys.*, 1987, **26**, pp. 1097–1101
7 MEIER, H. P., BROOM, R. F., EPPERLEIN, P. W., GIESON, E. V., HARDER, C., and JACKEL, H.: 'Problems related to the formation of lateral p–n junctions on channeled substrate (100) GaAs for lasers', *J. Vac. Sci. Technol.*, 1988, **B6**, pp. 692–695
8 WOOD, C. E. C., DESIMONE, D., SINGER, K., and WICKS, G. W.: 'Magnesium- and calcium-doping behaviour in molecular-beam epitaxial III-V compounds', *J. Appl. Phys.*, 1982, **53**, pp. 4230–4235

526.

320 fs SOLITON GENERATION WITH PASSIVELY MODE-LOCKED ERBIUM FIBRE LASER

Indexing terms: Lasers, Optical fibres

The generation of ultrashort 320 fs soliton pulses at 1560 nm from an all-fibre, passively mode-locked erbium fibre is reported. Repetition rates as high as 10 GHz have been observed demonstrating the device's potential as a telecommunication soliton source.

Rare earth doped optical fibres,[1] offering wide gain bandwidths provide an ideal medium for the generation of ultrashort optical pulses. The main body of research in mode-locked fibre lasers has centred on active mode-locking schemes incorporating fast amplitude[2] or phase modulators.[3] However, the large nonlinear effects obtainable in optical fibres makes passive mode locking of fibre lasers an attractive proposition.[4]

Recently an all-fibre, selfstarting, passive mode-locking scheme*,[5] has been demonstrated based on the nonlinear amplifying loop mirror (NALM).[6,7] The device is capable of both soliton[5] and 'square' pulse generation,* these being the pulse forms most readily switched by the NALM. The shortest pulses so far obtained are solitons of 2 ps duration.[5] We

* RICHARDSON, D. J., *et al.*: 'Self starting, passively mode-locked erbium fiber laser'. Submitted to CLEO 1991

report here 320 fs soliton pulses generated with a passively mode-locked erbium fibre laser.

The experimental setup is illustrated in Fig. 1. The dispersion of the fibres used ($NA = 0{\cdot}15$, cutoff wavelength = 950 nm) was $D = +5$ ps/nm/km. The isolator loop was of

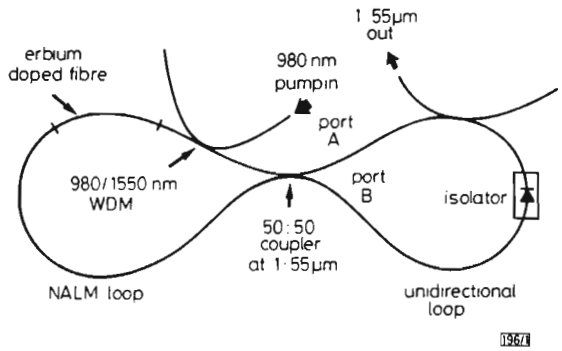

Fig. 1 *Experimental configuration of figure 8 mode-locking scheme*

length 8 m and the total NALM length varied between 8 and 36 m. The doped fibre, located asymmetrically within the NALM, had a length of 3 m and contained 800 ppm of Er^{3+}. The total excess loss of the cavity was estimated at 3 dB. The system was pumped with a Ti : sapphire laser operating at 980 nm. The output coupler gave 30% output coupling at 1550 nm. Polarisation controllers were included within both the NALM and isolator loops.

Both long duration >100 ps square pulse and soliton behaviours were observed with the system. The square pulses were generated at the cavity round trip frequency, the optical bandwidth of these pulses was 35 nm and the autocorrelation traces showed strong evidence of substructure on a 100 fs time scale. The substructure is thought to be due to the effect of modulational instability. At low pump powers (<100 mW) the square pulses became less stable and the system switched to the soliton regime of operation. In general the soliton pulses were seemingly randomly spaced within bunches, the bunches repeating at the cavity round trip frequency. An example of this random pulsing is shown in Fig. 2, where, because the detector response time is far longer than the pulse duration,

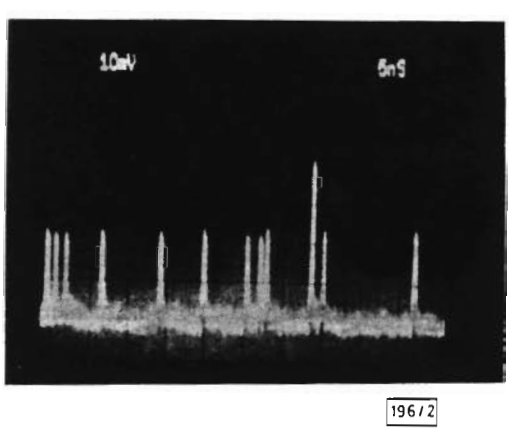

Fig. 2 *Typical internal structure of soliton pulse bunches generated at cavity round trip frequency*

Pulse of apparently twice amplitude of others is due simply to two pulses occurring within time period less than detector response time
Solitons were of 450 fs duration

the oscilloscope effectively displays the pulse energy (the pulse with twice the amplitude of the others is due to two pulses occurring within the detector response time). With appropriate adjustment of loop birefringence and input pump power, harmonic mode locking occurred (see Fig. 3). Repetition rates from 50 MHz to 10 GHz were observed within the bunches, and autocorrelation was required to measure the highest repetition rates. In a practical system addition of a pulse multiplier

such as Fabry–Perot cavity or a recirculating delay line might be needed to stabilise the repetition rate. A background free autocorrelation trace of the shortest pulses obtained is shown in Fig. 4. As is seen in the Figure the trace is extremely well fitted by a $\text{sech}^2\ \tau$ pulse form. The T_{FWHM} of the pulses was 320 fs. The corresponding optical spectrum, of width 9 nm, is

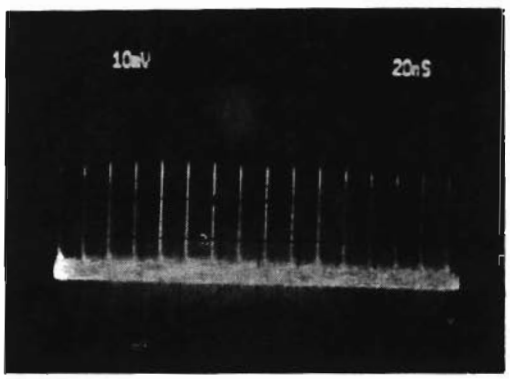

Fig. 3 *Harmonic mode locking of fibre laser, $f = 67{\cdot}2$ MHz*
Pulses have half width of 450 ps and peak power of 40 W
980 nm pump power was 50 mW

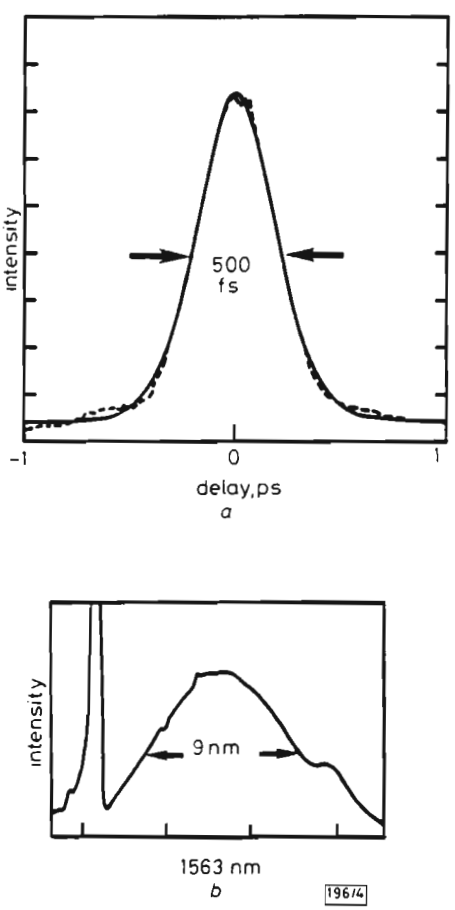

Fig. 4 *Background free autocorrelation trace and optical spectra of 320 fs soliton pulses*
Solid line autocorrelation profile represents nonlinear least squares fit to experimental data on assumption of $\text{sech}^2\ \tau$ pulse form
a Background free autocorrelation trace
b Optical spectra of 320 fs soliton pulses

also shown in Fig. 4, giving a time bandwidth product of 0·32 ($\Delta\nu\Delta\tau = 0{\cdot}315$ for a soliton). The estimated peak pulse power of 50 W is in good agreement with that expected for a fundamental soliton of duration 320 fs. The optical spectra of the pulses both reflected and switched by the NALM are shown in Fig. 5, these spectra were obtained from examination of the pulses counterpropagating in the isolator loop. The central spectral hump (the soliton) is much reduced in the reflected

by the NALM. The fine spectral structure is though to be due to fibre birefringence axis/polariser misalignment within the isolator.

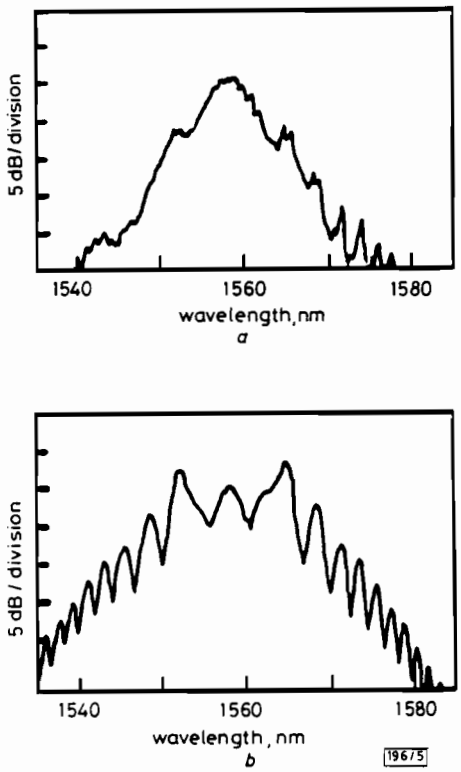

Fig. 5 *Optical spectra of pulses both switched and reflected by NALM during soliton regime operation of NALM*

Relative reduction of central hump in reflected trace clearly illustrates soliton switching characteristics of NALM
a Switched
b Reflected

We have demonstrated 320 fs soliton generation with a passively mode-locked fibre laser, at pump power levels attainable with diode lasers. In the future we anticipate locking the full 35 nm bandwidth of the erbium laser, this yielding a pulse width of 80 fs. In addition 10 GHz soliton repetition rates have been observed. The laser configuration is extremely attractive as a stable soliton source for future communication systems.

D. J. RICHARDSON
R. I. LAMING
D. N. PAYNE
M. W. PHILLIPS
V. J. MATSAS

Optoelectronics Research Centre, The University Southampton SO9 5NH, United Kingdom

15th February 1991

References

1 POOLE, S. B., PAYNE, D. N., and FERMANN, M. E.: 'Fabrication of low loss optical fibres containing rare earth ions', *Electron. Lett.*, 1985, **21**, pp. 737–738
2 KAFKA, J. D., BAER, T., and HALL, D. W.: 'Mode-locked erbium fibre laser', *Opt. Lett.*, 1989, **14**, pp. 1269–1271
3 FERMANN, M. E., *et al.*: 'Femtosecond fibre laser', *Electron. Lett.*, 1990, **23**, pp. 1737–1738
4 AVROMOPOLOUS, H. E., *et al.*: 'Passive mode-locking of an erbium fibre laser'. Topical meeting on optical amplifiers and their applications, Monterey, post deadline paper PDP8, 1990
5 DULING, I. N., III: 'All-fiber modelocked figure eight laser'. Optical Society of America, annual meeting, Boston, Post deadline paper, 1990
6 FERMANN, M. E., *et al.*: 'Non-linear amplifying loop mirror', *Opt. Lett.*, 1990, **15**, pp. 752–754
7 RICHARDSON, D. J., LAMING, R. I., and PAYNE, D. N.: 'Very low threshold Sagnac switch incorporating an erbium doped fibre amplifier', *Electron. Lett.*, 1990, **26**, pp. 1179–1181

DEPOLARISATION AND FIELD TRANSMITTANCES IN INDOOR COMMUNICATIONS

Indexing term: Microwave measurement

Measurements of copolar and crosspolar field amplitudes in an indoor cordless communications environment are presented. Measurements of narrowband and wideband transmittance magnitude are also presented for vertical and horizontal polarisations. An important longitudinal component is identified and the general concepts of co- and crosspolar (transversal and longitudinal) frequency/distance transmittance $H(j\omega, d)$ are introduced and defined.

Background: A particular type of mobile radio channel is the indoors communications environment. Because of fixed band allocations, the use of the frequency bandwidth for more or less adjacent picocells of less than 100 m in diameter is inevitable. Thus, the rate of decay of received power with distance from the indoors base station is attracting a great deal of attention (e.g. Reference 1). Description of the power level variability in various types of environments within a microcell can also be found and base station diversity is now being contemplated in addition to handset diversity.[2] Furthermore, dispersiveness can be important and several organisations and investigators are concerned in characterising it either in the time or in the frequency domain; the delay spread (e.g. Reference 3) and the 3 dB width of the frequency correlation function[1] are two ways of achieving this.

Complementary to the above studies is the understanding of the physical mechanisms which lead to a complex indoors multipath structure of the field. This is important because it leads to models which, it is hoped adequately reflect those physical processes. For example a simple model based on transmissions and reflections along a vertical plane in a multifloor building[4] can rapidly show the relative importance of

(1) the various multipath rays at the specified frequency range

(2) the transmitted polarisation

(3) the types of interfloor material used

The iteration modelling-experimental measurements results in

(*a*) better prediction of signal levels against distance and/or frequency (see below)

(*b*) selection of an adequate analytical channel transmittance model (2, 3 or more rays)[4]

(*c*) improved planning of additional or novel experimental measurements.

Measurements and definitions: The power-distance or amplitude/phase-frequency results found in the literature do not resolve the field structure seen by the portable or mobile receiver. The type of field polarisation is, however, important because the reflection coefficient depends not only on the incidence angle of the various rays and the materials of the interfloor, walls etc, but also on the state of polarisation of those incident rays. Therefore, a complex copolar and crosspolar field structure would be expected. Furthermore, for each polarisation received the corresponding channel transmittance $H(j\omega)$ would be expected.

To validate these concepts, preliminary experimental results were carried out in a microcell of an industrial building. Both transmitter and receiver antennas were $\lambda/4$ dipoles (sleeve antenna) operating at L band. The transmitter antenna was suspended from the ceiling and the receiver antenna could be moved horizontally at about 0·8 m height from the floor. The transmitter antenna could be oriented either vertically or horizontally. The receiver antenna could be oriented vertically, horizontally or longitudinally (i.e. in the direction of the baseline transmitter/receiver). The microcell environment was an electronics laboratory of 7 m × 10 m with a clear 10 m long and 3 m wide spacing along which the measurements were